Hindawi
Journal of Sensors
Volume 2017, Article ID 9671378, 8 pages
https://doi.org/10.1155/2017/9671378

Research Article

Modified FOA Applied to Parameter Extraction of Flux-Gate Core

Wenjuan Jiang,[1,2] Yunbo Shi,[1] and Wenjie Zhao[1]

[1] *The Higher Educational Key Laboratory for Measuring & Control Technology and Instrumentations of Heilongjiang Province, School of Measurement-Control Technology & Communications Engineering, Harbin University of Science and Technology, Harbin 150080, China*
[2] *School of Automation Engineering, Northeast Electric Power University, Jilin 132012, China*

Correspondence should be addressed to Yunbo Shi; shiyunbo@126.com

Received 17 September 2016; Revised 16 December 2016; Accepted 27 December 2016; Published 14 March 2017

Academic Editor: Pietro Siciliano

The accuracy of the magnetic core model is important to the analysis and design of the flux-gate sensor. The Jiles-Atherton model (J-A model) is the mostly used model to describe the hysteresis characteristics of the flux-gate core. But the parameters of J-A model are difficult to identify. In this paper, Fruit Fly Optimization Algorithm (FOA) is proposed to identify the parameters of the J-A model. In order to enhance the performance of the identification, a Modified Fruit Fly Optimization Algorithm (MFOA) is applied to extract the parameters of the flux-gate core. The effectiveness of MFOA is verified through five typical test functions. The influence of variation factor h on the performance of MFOA is discussed. The impact of variation factor h on parameters extraction of hysteresis loop is studied. It is shown that MFOA with appropriate selection of variation factor h will get better performance in the accuracy, stability, and simulation time compared to those of PSO and FOA.

1. Introduction

Flux-gate sensor is the best vector magnetic sensor with integrated performance [1]. The magnetic property of iron core material is an important factor that influences the characteristics of flux-gate. The accuracy of the mathematical model of the iron core material affects the accuracy of the flux-gate analysis. Jiles-Atherton model (J-A model) [2] is based on the physical process of hysteresis and has the merits of less parameters and simplicity in expression, which makes it mostly used in practice. But the parameters are sensitive to the hysteresis loop, so they are difficult to be determined.

Many methods have been proposed to determine the J-A model parameters, such as Genetic Algorithm (GA) [3], Particle Swarm Optimization (PSO) [4], Artificial Neural Network (ANN) [5], and Shuffled Frog Leaping Algorithm (SFLA) [6].

Literature [7] has proposed using Fruit Fly Optimization Algorithm (FOA) and Modified Fruit Fly Optimization Algorithm (MFOA) to identify the J-A model parameters and shows good performance. But it has not verified the effectiveness of the algorithm and analyzed the influence of the variation factor h on the performance of the MFOA. So the main contributions of this paper are as follows: (1) proposing using dynamic variable step size to modify FOA; (2) discussing the effectiveness of MFOA by tests on five typical functions; (3) analyzing the influence of variation factor h on the performance of MFOA; (4) applying the MFOA to extract the parameters of hysteresis loop and analyze the simulation results compared with PSO and FOA.

2. J-A Hysteresis Model

J-A hysteresis model is a mathematical model for describing the nonlinear characteristics of magnetic cores, which was proposed by Jiles and Atherton in 1986 [2]. J-A model is generated from the physical process of the magnetization M which is divided into irreversible magnetization component

M_{irr} caused by domain wall displacement and reversible magnetization component M_{rev} caused by domain wall bending. According to (1), the relationship between M and the magnetic field strength H can be described as (2):

$$\begin{aligned} M &= M_{\text{rev}} + M_{\text{irr}}, \\ M_{\text{rev}} &= c\left(M_{\text{an}} - M_{\text{irr}}\right), \\ \frac{\mathrm{d}M_{\text{irr}}}{\mathrm{d}H_e} &= \frac{1}{\delta k}\left(M_{\text{an}} - M\right), \\ H_e &= H + \alpha M, \\ M_{\text{an}} &= M_s \cdot \left\{\coth\left(\frac{H_e}{a}\right) - \left(\frac{a}{H_e}\right)\right\}, \end{aligned} \tag{1}$$

$$\frac{\mathrm{d}M}{\mathrm{d}H} = \frac{(1-c)\left(M_{\text{an}} - M\right) + ck\delta\left(\mathrm{d}M_{\text{an}}/\mathrm{d}H\right)}{\delta k - \alpha(1-c)\left(M_{\text{an}} - M\right)}. \tag{2}$$

Here, M_{an} is the anhysteretic magnetization. H_e is effective magnetic field. δ is +1 for $\mathrm{d}H/\mathrm{d}t > 0$ and −1 for $\mathrm{d}H/\mathrm{d}t \le 0$. The five parameters that need to be identified are as follows: pinning factor k, reversible magnetization coefficient c, coupling factor between magnetic domains α, form factor a, and saturation magnetization M_s.

3. MFOA and Its Performance

3.1. MFOA. Fruit Fly Optimization Algorithm (FOA) was put forward by Pan in 2012, which is described in detail in literature [8]. FOA uses fruit fly group collaboration mechanism and information sharing mechanism to search for the optimal solution, which causes it to have good ability of global optimization. Also the algorithm has the merits of simplicity, less parameters, small amount of calculation, and high precision, which makes it widely used in practical problems [9–11]. But when it encounters complex high dimension optimization problems, FOA may fall into local convergence with slow search speed, low efficiency, and poor stability.

In early stage of search, the fruit fly uses smell to search for food, which can help them to search for the position with greater concentration of fruit. In the later stage of search, it has certain blindness and gambling to determine the position of fruit fly, which results in a waste of resources, low efficiency, and poor accuracy.

In order to solve this problem, the dynamic variable step size is proposed. The direction of the movement of the fruit fly is determined by

$$\begin{aligned} X_{k+1} &= x\text{-axis} + \text{Random Value} * D_k * h^k, \\ Y_{k+1} &= y\text{-axis} + \text{Random Value} * D_k * h^k. \end{aligned} \tag{3}$$

Here, D_k is the distance between the optimal position of fruit fly for the kth iteration and the origin. Parameter h is variation factor which is in the range of [0.1, 10] according to different optimization problems.

3.2. Simulation Experiments and Results Analysis. In order to verify the effectiveness and advantages of the MFOA, five functions are used to test the algorithm in this paper. Functions f_1 and f_2 are the single-peak functions, and functions f_3–f_5 are multipeak functions. The five test functions are shown in Section 3.2.1. The simulation results are compared with those of the PSO algorithm and the original FOA.

3.2.1. Test Functions

(1) f_1 – *Sphere Model*

$$f_1(x) = \sum_{i=1}^{n} x_i^2, \quad -100 \le x_i \le 100,\ \min f_1(x) = f_1(0,\ldots,0) = 0 \tag{4}$$

(2) f_2 – *Exponential Function*

$$f_2(x) = \exp\left(0.5\sum_{i=1}^{n}|x_i|\right) - 1, \quad -1.28 \le x_i \le 1.28,\ \min f_2(x) = f_2(0,\ldots,0) = 0 \tag{5}$$

(3) f_3 – *Ackley Function*

$$f_3(x) = -20\exp\left[-0.2\sqrt{\frac{1}{n}\sum_{i=1}^{n}x_i^2}\right] - \exp\left[\frac{1}{n}\sum_{i=1}^{n}\cos 2\pi x_i\right] + 20 + e, \quad -32 \le x_i \le 32,\ \min f_3(x) = f_3(0,\ldots,0) = 0 \tag{6}$$

(4) f_4 – *Griewank Function*

$$f_4(x) = \frac{1}{4000}\sum_{i=1}^{n}x_i^2 - \prod_{i=1}^{n}\cos\left(\frac{x_i}{\sqrt{i}}\right) + 1, \quad -600 \le x_i \le 600,\ \min f_4(x) = f_4(0,\ldots,0) = 0 \tag{7}$$

(5) f_5 – *Rastrigin Function*

$$f_5(x) = \sum_{i=1}^{n}\left[x_i^2 - 10\cos\left(2\pi x_i\right) + 10\right], \quad -5.12 \le x_i \le 5.12,\ \min f_5(x) = f_5(0,\ldots,0) = 0. \tag{8}$$

3.2.2. Simulation Experiments and Results Analysis. In simulations, the dimension of the five test functions is 30, and maximum number of iterations is 3000, variation factor h of MFOA is 2, and the inertia factor and the acceleration constants of PSO are $\eta = 0.75$, $c_1 = 2$, and $c_2 = 2.5$, respectively.

The optimal value, the average value of 20 times, variance, and running time are shown in Table 1.

Table 1: Simulation results for three methods.

Function	Method	Optimal value	Mean value	Variance	Time/s
f_1	PSO	$1.535e-5$	$8.729e-5$	$7.584e-9$	1.549
	FOA	$2.177e-6$	$2.418e-1$	$1.196e-1$	4.164
	MFOA	$2.083e-307$	$3.922e-307$	0	14.48
f_2	PSO	$2.836e-4$	0.182	0.136	1.864
	FOA	$4.045e-3$	$4.034e-1$	3.190	4.285
	MFOA	0	0	0	12.08
f_3	PSO	$3.191e-4$	$7.484e-4$	$5.902e-8$	2.611
	FOA	$1.081e-3$	$6.061e-1$	$4.777e-1$	4.617
	MFOA	0	0	0	12.37
f_4	PSO	$1.920e-4$	$2.182e-2$	$5.253e-4$	2.964
	FOA	$1.446e-7$	$4.819e-2$	$5.311e-3$	5.057
	MFOA	0	0	0	12.86
f_5	PSO	1.059	$2.463e+1$	$1.128e+2$	2.104
	FOA	$4.340e-4$	$8.374e-1$	$5.193e-1$	4.575
	MFOA	0	0	0	12.35

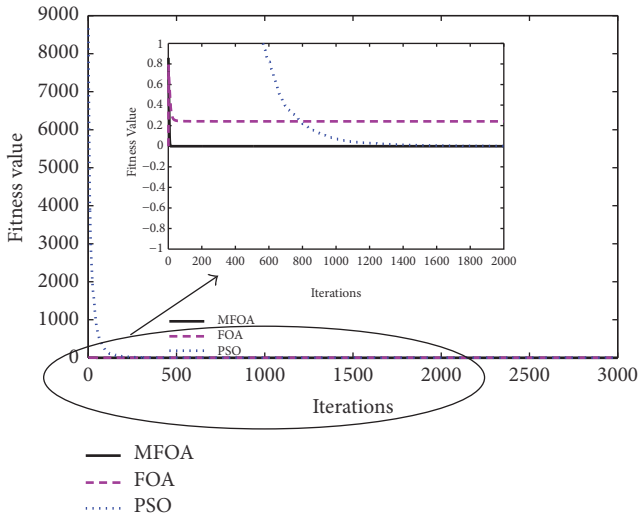

Figure 1: Optimization process of f_1.

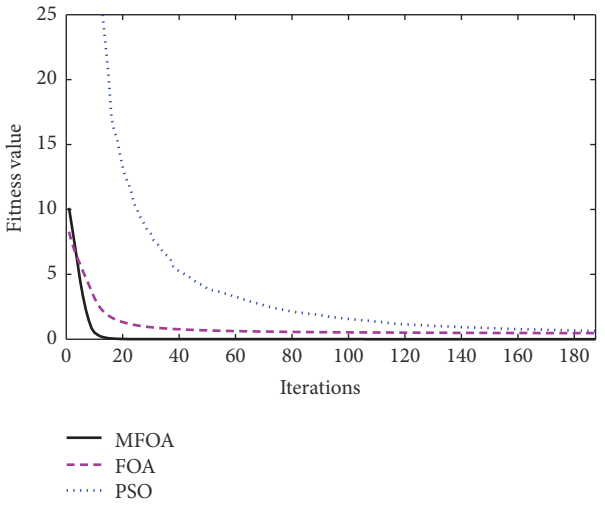

Figure 2: Optimization process of f_2.

From Table 1, the following can be seen: (1) running time: the running time of PSO algorithm is the shortest, and the running time of MFOA is the longest which is about 6 times that of PSO and about 3 times that of FOA; (2) the precision of the algorithm: MFOA has the highest accuracy which is far higher than the FOA and PSO algorithm; (3) variance: the variance values of MFOA for the five test functions are all 0, which states that MFOA has the best stability, FOA for single-peak function also shows instability, and PSO for multipeak function f_5 is unstable. During operations, PSO algorithm and FOA are easy to fall into local convergence, especially for multipeak function f_5.

The optimization process of the five test functions for three algorithms is shown in Figures 1–5. Figure 1 shows function value with iterations for function f_1 with partially enlarged detail. In order to see the process clearly, Figures 2–4 are the partially enlarged detail figures. From Figures 1–5, it can be seen that MFOA has best convergence precision and stability. The optimization precision and stability of PSO algorithm are higher than those of FOA expect f_5 but much lower than MFOA; PSO and FOA methods show instability and low precision for complex multipeak function f_5.

In the iterative process, the location search of fruit flies using dynamic variable step size makes fruit flies search in a wider range and improves the diversity and development of fruit flies' positions, which can help the algorithm escape from local optimal and improve the precision of the algorithm.

So MFOA has high convergence precision and strong ability to jump out of local extreme value. To ensure the capability of algorithm to jump out of the extreme, fruit flies are needed to search the best position in a wider range, so the simulation time for 3000 iterations of MFOA is longer than that of FOA.

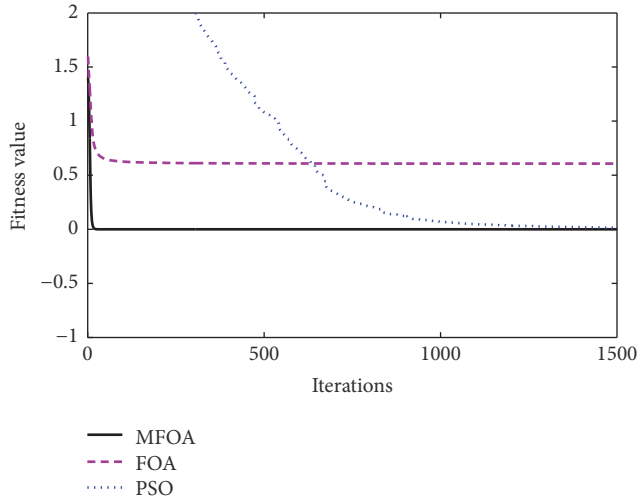

Figure 3: Optimization process of f_3.

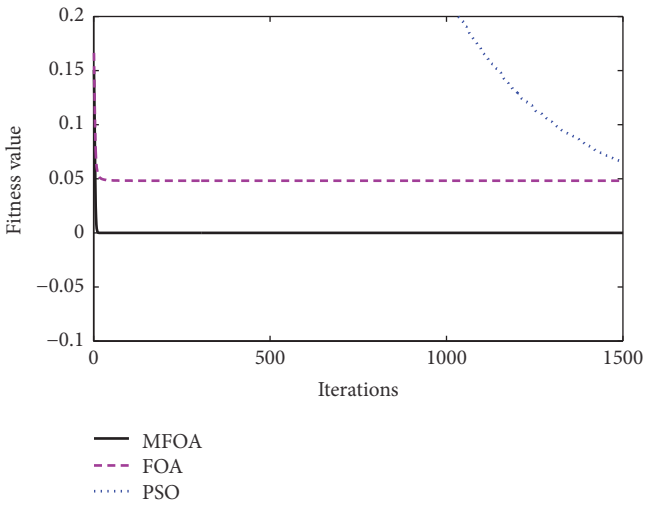

Figure 4: Optimization process of f_4.

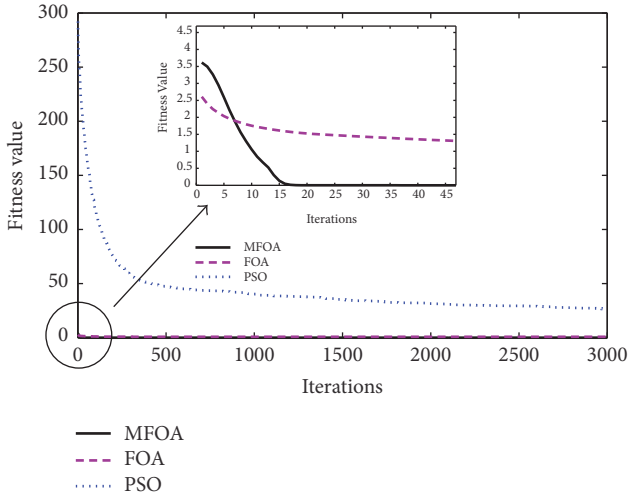

Figure 5: Optimization process of f_5.

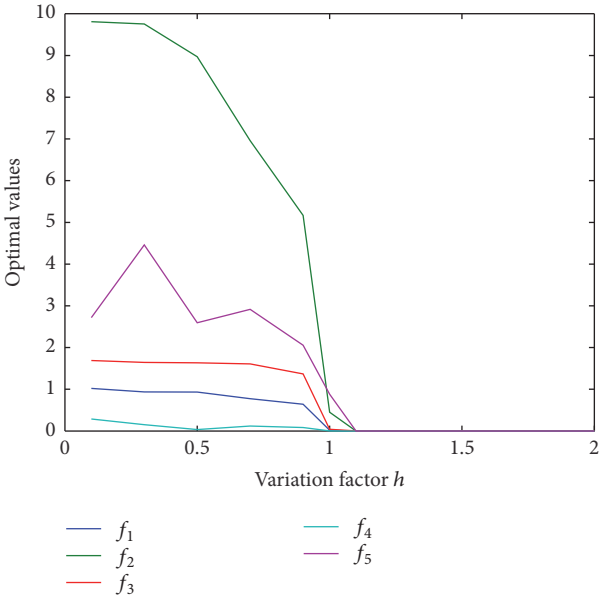

Figure 6: Optimal value with h for five functions.

The factors that influence the performance of MFOA are population size, the maximum number of iterations, and the variation factor h. In this paper, simulations have been performed to study the influence of the parameter h. For each test function, the MFOA method is used to find the optimal solutions at $h = [0.1, 0.3, 0.5, 0.7, 0.9, 1, 1.1, 1.3, 1.5, 2]$ and the algorithm runs for 20 times for each h. The curves of average optimal value with h for five test functions are shown in Figure 6, the curves of variance with h are shown in Figure 7, and the curves of simulation time with h are depicted in Figure 8.

From Figure 6, the following is found: (1) the optimal values decrease with the increase of h; (2) when $h \in [0.1, 0.9]$, the algorithm has poor precision, and when $h > 1$, the algorithm has better precision; (3) the bigger h value is, the better the precision is; (4) when h achieves some value, the optimal value changes little.

From Figure 7, the following is shown: (1) the variance decreases with the increase of h; (2) when $h > 1$, the algorithm has better stability; (3) the bigger h value is, the better the stability is; (4) when h achieves some value, the variance tends to 0.

From Figure 8, it can be seen that when $h \in [0.1, 1.1]$, the simulation time is almost the same, but when $h > 1.3$, the simulation time is increasing quickly with h.

From the analysis above, the following is stated: (1) when $h = 1.1$, the algorithm has better precision, better stability, and better convergence rate; (2) bigger h has better precision and stability, but the simulation time increases at the same time when $h > 1.3$.

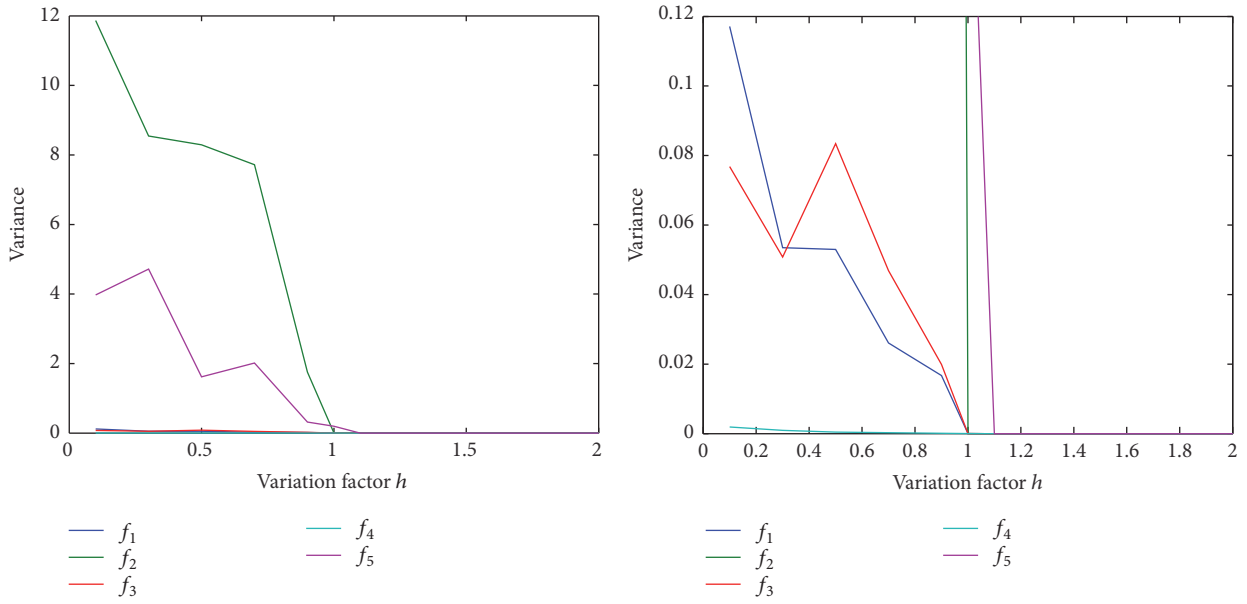

(a) Full picture (b) Partially enlarged picture

Figure 7: Variance with h for five functions.

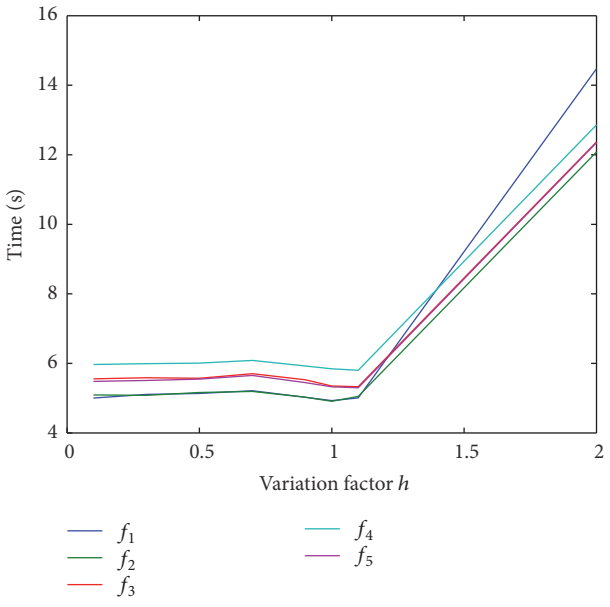

Figure 8: Simulation time with h for five functions.

4. Parameters Extraction of J-A Model

The fitness function in this paper is as follows:

$$\text{fitness} = \frac{1}{N}\sqrt{\sum_{i=1}^{N}\left(B_{\text{cal}i} - B_i\right)^2}. \quad (9)$$

Here, $B_{\text{cal}i}$ is the calculated value of $B(H_i)$ and B_i is experimental data at H_i.

4.1. Diagram. Figure 9 is the diagram of the parameters extraction of J-A model applying MFOA.

4.2. Parameters Extraction of J-A Model

4.2.1. The Influence of Factor h on the Extraction Result. From Section 3.2.2, it can be seen that the factor h influences the performance of the MFOA. Therefore, the influence of the factor h on the extraction performance has been discussed in this section. Here, h = [0.1, 0.3, 0.5, 0.7, 0.9, 1.1, 1.3, 1.5, 2, 3, 4, 5, 6, 7, 8, 9, 10]. Figures 10–12 show the curves of fitness value, variance, and simulation time with h, respectively.

From Figure 10, the following can be found: (1) when $h \in [0.1, 0.7]$, the fitness value decreases with the increase of h; (2) when $h > 1.1$, the fitness value increases; (3) when $h = 0.9$, the fitness value (0.005 T) is the best. From Figure 11, the following can be seen: (1) when $h = 0.7$, $h = 0.9$, and $h = 1.1$, the variances are the smallest, which are 3.44×10^{-6}, 2.59×10^{-6}, and 2.55×10^{-6}, respectively; (2) when $h > 1.3$, the variance is increased with the increase of h. Figure 12 shows the following: (1) when $h \in [0.1, 0.9]$, the simulation time increases with the increase of h; (2) when $h > 2$, the simulation time changes in a small way, which is about 130 s. So it is stated that when $h = 0.9$, the MFOA has good extraction performance in accuracy, stability, and simulation time.

4.2.2. Parameters Setting. MFOA, FOA, and PSO are used to identify the parameters of J-A model according to the experimental hysteresis loop of the nonoriented steel V3250-50A taken from literature [3]. The parameters of PSO algorithm are set according to literature [12]: swarm size 100, inertial factor 0.75, and acceleration constants $c_1 = 2$ and $c_2 = 2.5$.

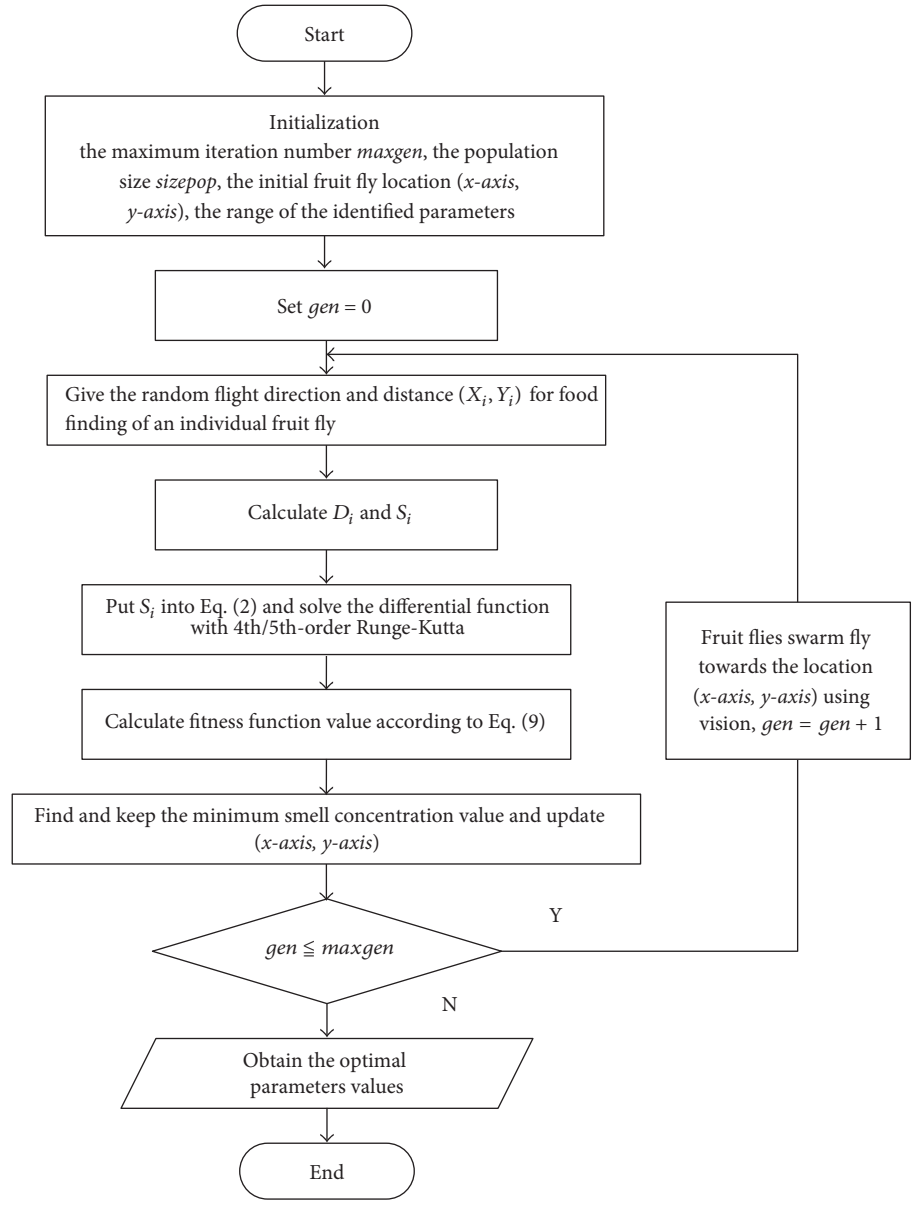

Figure 9: The implementation procedure of MFOA.

The swarm size of FOA and MFOA is also set to 100. The variation factor h of MFOA is 0.9 according to Section 4.2.1. The maximum iterations for three methods are all 50.

4.2.3. Simulation Results and Analysis. The parameters of J-A model obtained by three methods are as follows:

(1) MFOA: $M_s = 1.2426 \times 10^6$, $a = 63.86$, $\alpha = 11.79 \times 10^{-5}$, $c = 0.77$, $k = 60.97$.

(2) FOA: $M_s = 1.2446 \times 10^6$, $a = 51.26$, $\alpha = 9.076 \times 10^{-5}$, $c = 0.34$, $k = 66.70$.

(3) PSO: $M_s = 1.2312 \times 10^6$, $a = 71.55$, $\alpha = 11.89 \times 10^{-5}$, $c = 0.53$, $k = 69.22$.

Figure 13 depicts the hysteresis loops according to the parameters obtained. The errors between calculated data and measured data for three methods are shown in Figure 14, which gives the part when $dH/dt > 0$. The blue dot line (obtained by PSO) shows the error is small when the hysteresis loop is becoming saturated, and the biggest error −0.205 T is obtained at $H = 100$ A/m. The green line (obtained by FOA) shows the biggest error is −0.1507 T at $H = 6.75$ A/m and the error is bigger than that of MFOA and PSO when H is becoming saturated. The red line (obtained by MFOA) shows the biggest error is 0.09 T at $H = -100$ A/m and the error is bigger than that of PSO when H is becoming saturated.

Table 2 shows convergence values of fitness function (the best, worst, and mean), variance, and simulation time. From Table 2, it can be observed that the fitness value achieved by MFOA is better than the minimum fitness values achieved

Table 2: The results of convergence values.

Methods	Best	Worst	Mean	Variance	Time/s
PSO	0.0125	0.0589	0.0279	$2.976e-4$	4932
FOA	0.0060	0.0286	0.0086	$4.973e-5$	150
MFOA	0.0039	0.0079	0.0050	$2.590e-6$	137

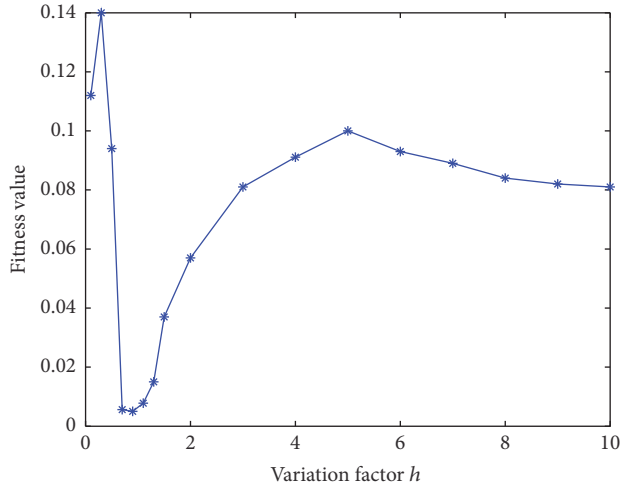

Figure 10: Fitness value with h for parameters extraction of J-A model.

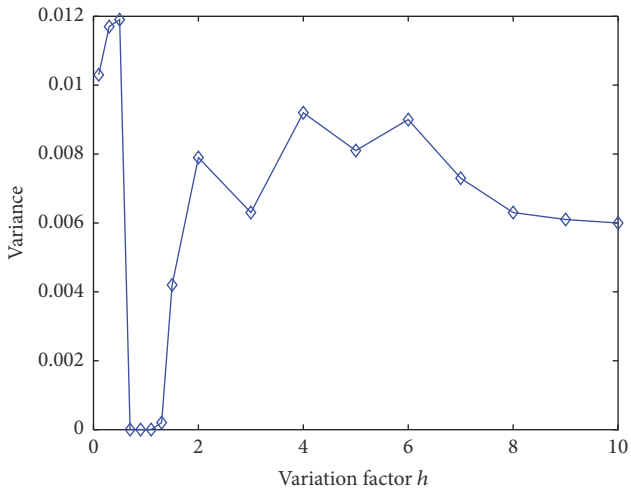

Figure 11: Variance with h for parameters extraction of J-A model.

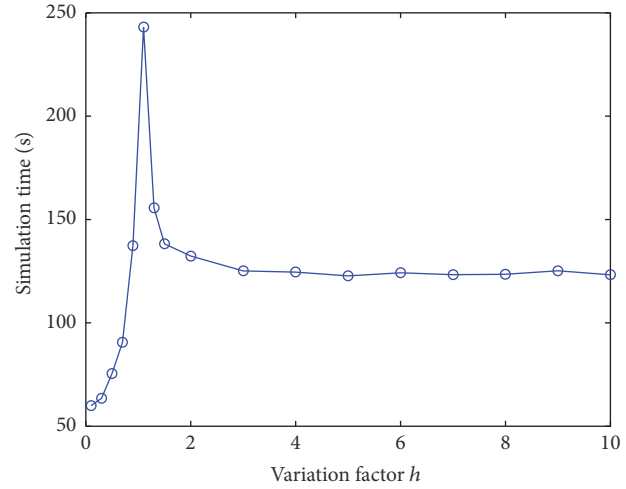

Figure 12: Simulation time with h for parameters extraction of J-A model.

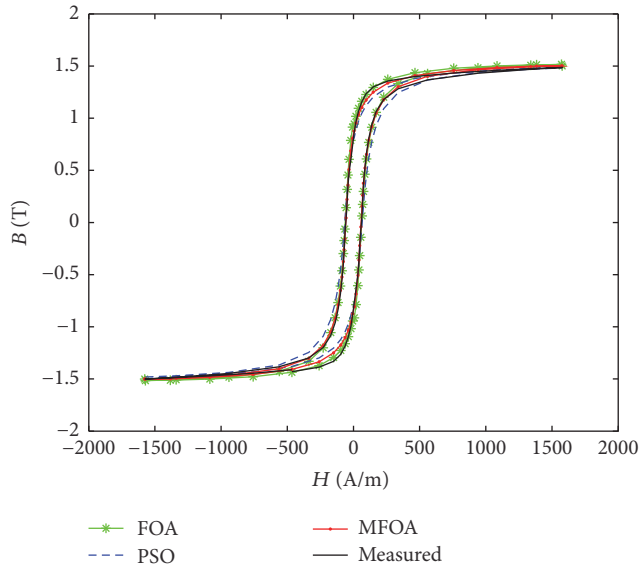

Figure 13: Calculated and measured B-H curves.

by PSO and FOA. The precision of MFOA is the best of the three methods. The variance of the convergence values for 20 times obtained by MFOA is 2.590×10^{-6} which is the smallest of the three methods. The smaller the variance is, the better the stability of the algorithm is. So the stability of MFOA is much better than that of FOA and PSO. The simulation time for PSO is much longer than that of FOA and MFOA.

5. Conclusions

In this paper, a modified FOA is proposed and the effects of the variation factor h of MFOA are studied through five test functions. The results show that the variation factor h of MFOA has important influence on the accuracy, stability, and simulation time of the algorithm. The reasonable selection of h can improve the comprehensive performance of the

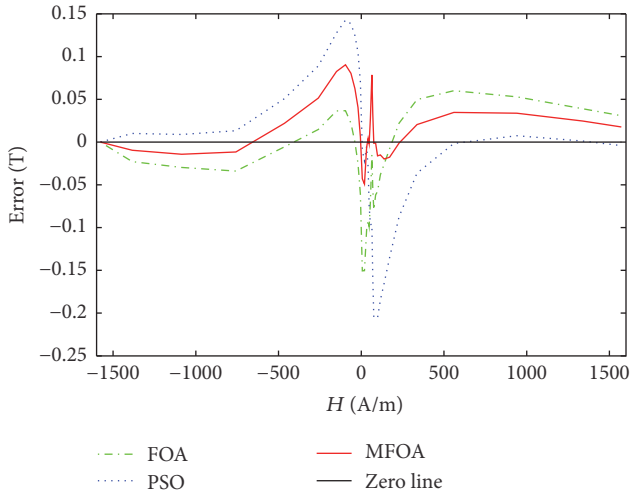

FIGURE 14: Error curves of three methods when $dH/dt > 0$.

algorithm. FOA and MFOA are applied to optimize the parameters of J-A model. The simulation results show that MFOA with reasonable selection of h is better than PSO and FOA in precision and stability.

In this paper, the parameters of J-A model are extracted from static hysteresis loop. But the hysteresis loop varies with the changes of temperature and the frequency of the excitation magnetic field. So more work should be done on the following: (1) the improvement of J-A model with temperature and frequency; (2) parameters extraction of the improved J-A model.

Conflicts of Interest

The authors declare no conflicts of interest.

Authors' Contributions

Yunbo Shi and Wenjie Zhao proposed the new method to extract the parameters of J-A model; Wenjuan Jiang wrote simulation programs, performed data analysis, and wrote the paper. All the authors were involved in the paper preparing.

Acknowledgments

This work was supported by the National Natural Science Foundation of China (no. 61501149 and no. 31401569), the Science and Technology Development Plan of Jilin Province (no. 20150520135JH), and the Science and Technology plan of Jilin City (2015640100).

References

[1] P. Ripka and M. Janošek, "Advances in magnetic field sensors," *IEEE Sensors Journal*, vol. 10, no. 6, pp. 1108–1116, 2010.

[2] D. C. Jiles and D. L. Atherton, "Theory of ferromagnetic hysteresis," *Journal of Magnetism and Magnetic Materials*, vol. 61, no. 1-2, pp. 48–60, 1986.

[3] K. Chwastek and J. Szczyglowski, "Identification of a hysteresis model parameters with genetic algorithms," *Mathematics and Computers in Simulation*, vol. 71, no. 3, pp. 206–211, 2006.

[4] R. Marion, R. Scorretti, N. Siauve, M.-A. Raulet, and L. Krähenbühl, "Identification of jiles-Atherton model parameters using particle swarm optimization," *IEEE Transactions on Magnetics*, vol. 44, no. 6, pp. 894–897, 2008.

[5] D. Grimaldi, L. Michaeli, and A. Palumbo, "Automatic and accurate evaluation of the parameters of a magnetic hysteresis model," *IEEE Transactions on Instrumentation and Measurement*, vol. 49, no. 1, pp. 154–160, 2000.

[6] R.-A. Naghizadeh, B. Vahidi, and S. H. Hosseinian, "Parameter identification of Jiles–Atherton model using SFLA," *COMPEL—The International Journal for Computation and Mathematics in Electrical and Electronic Engineering*, vol. 31, no. 4, pp. 1293–1309, 2012.

[7] W. J. Jiang, Y. B. Shi, W. J. Zhao, and X. X. Wang, "The parameters identification of magnetic core using fruit fly optimization algorithm," *Chemical Engineering Transactions*, vol. 51, pp. 169–174, 2016.

[8] W.-T. Pan, "A new fruit fly optimization algorithm: taking the financial distress model as an example," *Knowledge-Based Systems*, vol. 26, pp. 69–74, 2012.

[9] X. Li, L. Sun, and M. Yang, "Research on ultrasonic signal processing based on improved FOA matching pursuit," *Chinese Journal of Scientific Instrument*, vol. 34, no. 9, pp. 2068–2073, 2013 (Chinese).

[10] J.-Q. Li, Q.-K. Pan, and K. Mao, "A hybrid fruit fly optimization algorithm for the realistic hybrid flowshop rescheduling problem in steelmaking systems," *IEEE Transactions on Automation Science and Engineering*, vol. 13, no. 2, pp. 932–949, 2016.

[11] Y. Zhang, G. Cui, Y. Wang, X. Guo, and S. Zhao, "An optimization algorithm for service composition based on an improved FOA," *Tsinghua Science and Technology*, vol. 20, no. 1, pp. 90–99, 2015.

[12] W. Wang, C. Lin, and Y. Zheng, "Experiment and analysis of parameters in particle swarm optimization," *Journal of Xihua University*, vol. 27, pp. 76–80, 2008 (Chinese).